

pH effect on the synthesis of different size silver nanoparticles evaluated by DLS and their size-dependent antimicrobial activity

Efeito do pH na síntese de diferentes tamanhos de nanopartículas de prata avaliados por EDL e sua atividade antimicrobiana dependente do tamanho

Leiriana Aparecida Pinto Gontijo¹, Ellen Raphael^{1,2},
Daniela Pereira Santos Ferrari¹, Jefferson Luis Ferrari¹,
Juliana Pereira Lyon¹, Marco Antônio Schiavon¹

¹ Grupo de Pesquisa em Química de Materiais - (GPQM), Departamento de Ciências Naturais, Universidade Federal de São João del-Rei, Campus Dom Bosco, Praça Dom Helvécio, 74, CEP: 36301-160, São João del-Rei, MG, Brazil.

² Escola Superior de Tecnologia, Engenharia Química, Universidade Estadual do Amazonas, Avenida Darcy Vargas, 1200, CEP: 69050-020, Manaus, AM, Brazil.

e-mail: leiriana@hotmail.com, eraphael@uea.edu.br, dapesantos@gmail.com, jeffersonferrari@gmail.com, julianalyon@ufsj.edu.br, schiavon@ufsj.edu.br

ABSTRACT

This paper reports citrate-stabilized silver nanoparticles (AgNPs) synthesized by nitrate ion chemical reduction with sodium borohydride, at different pHs (2–9). The AgNPs synthesized by this method exhibited size distribution from 5 to 249 nm, depending on pH, as determined by dynamic light scattering, and morphology spherical, as determined by transmission electron microscopy. In pH range 3–7 occurred aggregation of the nanoparticles. The size distribution depending on pH was determined by dynamic light scattering. The zeta potential was determined, and the colloidal stability was correlated with nanoparticles aggregation at different pHs. The size-dependent antimicrobial activity was evaluated for two solutions, wherein both samples exhibited antimicrobial activity, although the smallest AgNPs without agglomeration have enhanced antimicrobial properties.

Keywords: Silver Nanoparticles, Zeta Potential, Dynamic Light Scattering, Size Distribution, Antimicrobial Activity.

RESUMO

Este trabalho relata nanopartículas de prata estabilizadas com citrato (AgNPs) sintetizadas pela redução química do íon nitrato com boro-hidreto de sódio, em diferentes pHs (2-9). As AgNPs sintetizadas por este método apresentaram distribuição de tamanho de 5 a 249 nm dependente do pH, conforme determinado por espalhamento dinâmico de luz, além de morfologia esférica, conforme determinado por microscopia eletrônica de transmissão. Na faixa de pH de 3 a 7 ocorreu a agregação das nanopartículas. A distribuição de tamanho, dependendo do pH, foi determinada por espalhamento dinâmico de luz. O potencial Zeta foi determinado e a estabilidade coloidal foi correlacionada com a agregação de nanopartículas em diferentes pHs. A atividade antimicrobiana dependente do tamanho foi avaliada para duas soluções, em que ambas as amostras exibiram atividade antimicrobiana, embora as menores AgNPs sem aglomeração apresentaram propriedades antimicrobianas melhores.

Palavras-chave: Nanopartículas de Prata, Potencial Zeta, Espalhamento Dinâmico de Luz, Distribuição de Tamanhos, Atividade antimicrobiana.

1. INTRODUÇÃO

Metal nanoparticles have attracted great interest in several areas, such as chemistry, physics, biology, and materials engineering. Among noble-metal nanoparticles, silver nanoparticles (AgNPs), has been widely studied due to their different physical, electronic, mechanical and chemical characteristics, such as high surface area/volume ratio, which stands out because it is not found in conventional materials and allows unusual applications of these materials, such as consumables, including soaps, toothpaste, and textile industries [1-3].

The AgNPs can be synthesized by different methods, such as the chemical reduction of metal ions in aqueous solutions, with or without stabilizing [4], or using the thermal decomposition of metal compounds in organic solvents [5]. Each synthesis route leads to peculiarities in the results related to morphology and size, producing nanoparticles spherical, elliptical, cubic, cylindrical, in the form of discs, dendrites, rods or wires, with different size dispersions [5-7]. The process involving the reduction of silver salts in an appropriate medium has been reported in the literature using various reducing agents, such as sodium borohydride [8], hydrazine hydrate [9], sodium citrate [10], and ascorbic acid [11]. In a reducing environment, some syntheses use a surface stabilizer and other are based only on reducing AgNO_3 with sodium borohydride (NaBH_4). In the case of routes without using surface stabilizer, smaller nanoparticles are formed, which are less stable over time [10-12]. The use of ligands allows obtaining larger nanoparticles; however, they are more stable over time [13-15]. The choice of a suitable ligand is extremely important for obtaining every type of nanoparticle [6]. Sodium citrate is the most commonly used stabilizer; it has the advantage of being compatible with biomolecules and can easily be exchanged on the other ligand [7]. The methods using sodium citrate are quite simple, effective, the synthesis is rapid, and is characterized by the appearance of a yellow color; however, one must take extreme care with the conditions because the AgNPs formed in this conditions, different from other stabilizers, are very unstable [2, 7].

Different routes presented in the literature show that the metallic AgNPs have different morphologies and sizes, being strongly influenced by synthesis route, as well as their final properties [3, 5, 16]. There are recent studies in the literature about pH and size-effect, which show that the dissolution of AgNPs depends on the medium [17, 18], and the nanoparticles size are directly affected by the pH adjusted, this pH influences in the size-effect can be observed by the colors, from colorless to yellow [19-21]. However, there no found studies reporting the use of the Dynamic Light Scattering (DSL) technique with Zeta potential measurements to evaluate this pH effect on the size and stability of nanoparticles formed by the sodium borohydride reduction method using sodium citrate as a stabilizing agent. So the DSL results of silver nanoparticles prepared with a very simple synthesis method, stabilized with citric acid, at different pHs, correlating their aggregation with the Zeta potential, are discussed in the present study.

A common AgNPs application is because they have activity against Gram-positive and Gram-negative bacteria, viruses, yeasts and filamentous fungi. Studies on AgNPs have attracted great interest; one of the reasons for these studies is the increase in antibiotic-resistant bacteria [1, 4]. The AgNPs present a broad-spectrum bactericidal action due to the presence of silver, which leads to numerous applications of this material. Furthermore, the relatively low cost of manufacturing these nanoparticles should be noted.

The antibacterial efficacy of these nanoparticles is another important focus in the studies on AgNPs, some papers reported the dependence of the bacterial activity with regard to the size of these nanoparticles [22, 23]. In this work, AgNPs were prepared from aqueous silver nitrate (AgNO_3) solution using sodium borohydride (NaBH_4) as the reductant and sodium citrate ($\text{Na}_3\text{C}_6\text{H}_5\text{O}_7$) as the stabilizer; the reduction method was used in aqueous media, as a simple route in the AgNPs preparation. Besides that, the influence of the pH was studied, and the antibacterial activity depending on the size of the Ag nanoparticles was evaluated against two different bacteria: Gram-negative (*Escherichia coli*) and Gram-positive (*Staphylococcus aureus*) and a fungus (*Candida albicans*).

2. MATERIALS AND METHODS

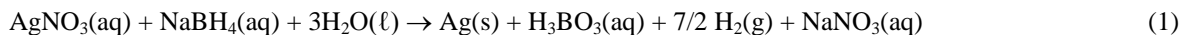
2.1 Materials

Silver nitrate (AgNO_3) and sodium borohydride (NaBH_4 , 97%) were obtained from Sigma-Aldrich (St. Louis, MO, USA), sodium citrate ($\text{Na}_3\text{C}_6\text{H}_5\text{O}_7$), nitric acid (HNO_3), and sodium hydroxide (NaOH) were obtained from Synth. All of the chemicals were used without additional purification. Milli-Q grade deionized water (Millipore) was used for the preparation of the solutions. Two bacterial strains, one Gram negative, namely *Escherichia coli* ATCC 53338, another one Gram positive, namely *Staphylococcus aureus* ATCC 29373, and a fungus strain, *Candida albicans* ATCC 10231, obtained from the Oswaldo Cruz Foundation,

were subjected to this analysis. The nutrient medium used was Sabouraud, from HiMedia Laboratories, with bacteriological agar as a solidifying agent.

2.2 Synthesis of AgNPs

The AgNPs synthesis was performed based on a previously reported method [24]. Silver nitrate (AgNO_3) were reduced via sodium borohydride (NaBH_4), to obtain metallic silver (Ag^0), according to reaction (1):



During the process, $\text{Na}_3\text{C}_6\text{H}_5\text{O}_7$ was used as an additive to prevent the aggregation of particles. In this way, 8.7 mL Milli-Q water was added to a beaker with 10 mL of AgNO_3 (4.0×10^{-4} M) and 0.5 mL of $\text{Na}_3\text{C}_6\text{H}_5\text{O}_7$ (4.0×10^{-2} M). Then 0.8 mL of NaBH_4 was added under stirring (5.0×10^{-2} M) and the solution was kept stirring for 15 min, controlling the pH in the range 2–9 as required, with HNO_3 (0.1 M) and NaOH (0.1 M).

2.3 Characterization of AgNPs

UV-vis absorption spectra were acquired on a Shimadzu UV-2550 spectrophotometer. The absorption measurements were performed with 10 mm quartz cuvettes (Shimadzu) using air-saturated solutions at room temperature, in the range 200–600 nm. The optical characterization was performed at room temperature and under ambient conditions without any post-preparative treatment to the as-prepared AgNPs.

The zeta potential (ζ) and the particle size distribution of the aqueous dispersions was determined by dynamic light scattering (DLS) using a Delsa Nano 2.31 apparatus from Beckman Coulter. DLS technique consists in the measurement of the time-dependent fluctuations in the intensity of light scattered by particles, which are in constant Brownian motion and relates this to the particle size; these stems from the fact that a small particle illuminated by a light source scatters light in all directions. Transmission electron microscopy (TEM) images of the AgNP samples were taking using a JEOL microscope JEM 2100 FEG-TEM operating at 200 kV. The as-prepared samples were diluted several times before dropping them onto ultrathin carbon-coated copper grids of 400 mesh, the excess solvent being previously evaporated.

2.4 Analysis of the antimicrobial activity of AgNPs

The antimicrobial effect of two different AgNP solutions, prepared at pH 4 and 9, on Gram-negative (*Escherichia coli*) and Gram-positive (*Staphylococcus aureus*) bacteria and on a fungus (*Candida albicans*) was investigated by the Zone of Inhibition (ZOI) in the disk diffusion test. The nutrient medium used was Sabouraud, which is composed of 10 g L^{-1} of peptone and NaCl , and 5 g L^{-1} of yeast extract supplemented with 16 g L^{-1} of bacteriological agar as a solidifying agent.

Silver-impregnated disks were prepared by loading Whatman filter papers (5 mm diameter) with AgNP solutions. AgNP impregnated filter papers were left to dry. The bacterial suspension (200 μL) was applied uniformly on the surface of a nutrient Sabouraud agar growth plate and the disks were gently placed on top of the agar. Plates with a clean filter paper, without AgNPs, were used as controls. The plates were incubated for 24–48 h at 37 °C, after which digital images of the plates were captured and the inhibition zone surrounding the disks was determined.

3. RESULTS AND DISCUSSION

3.1 Synthesis of Nanoparticles

Chemical reduction of AgNO_3 (4.0×10^{-4} M) was performed with NaBH_4 (5.0×10^{-2} M) as reduction agent. Initially, the nucleation of nanoparticles occurred by means of an inducing process starting from a supersaturated solution forming AgNP cores. From the core formed the nanoparticles were grown by a diffusion process. Prior to the NaBH_4 addition, $\text{Na}_3\text{C}_6\text{H}_5\text{O}_7$ (4.0×10^{-2} M) was added, as stabilizer agent, to prevent the AgNPs aggregating over time. Immediately after the reduction, the pH was controlled by dropping HNO_3 (0.1 M) and NaOH (0.1 M), under stirring to obtain eight solutions at different pH values, then the stability study of AgNPs was conducted according to pH variation. Figure 1 shows AgNP solutions, prepared in a first moment, at pH $8.9 + 0.15$, $4.2 + 0.10$, and $2.3 + 0.32$, the yellow color of the solution at pH $8.9 + 0.15$ is characteristic of formation of AgNPs, whereas the case of solutions with pH $4.2 + 0.10$ and $2.3 + 0.32$, exhibiting gray coloring indicates AgNPs aggregation.

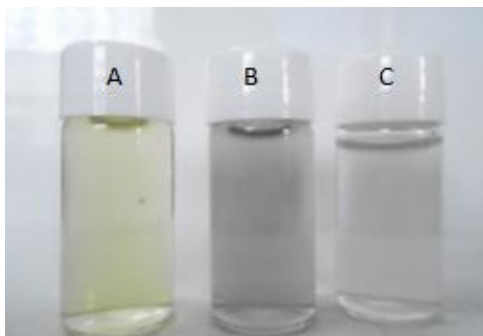


Figure 1: AgNP solutions prepared at pH = 8.9 + 0.15 (a), 4.2 + 0.10 (b), and 2.3 + 0.32 (c).

3.2 Characterization by Spectroscopy

UV-vis spectroscopy is a quick method for preliminary characterization of AgNPs that can be used to relate size parameters, shape, electron density, and other properties. These parameters are related to the optical absorption band, the maximum value of optical absorption (A_{max}), the wavelength of maximum absorption (λ_{max}) and the full width at half height (FWHH) [15]. Figure 2 shows the UV-vis spectra of AgNP samples prepared at different pH values.

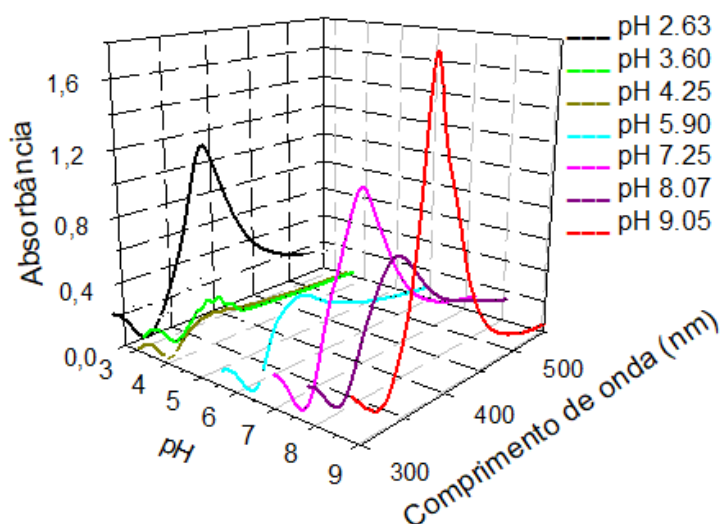


Figure 2: UV-vis spectra of AgNPs at different pHs.

The Figure 2 spectra shows a band around 390 nm, which is due to AgNPs surface plasmon resonance [24, 25]. The single band is an indication of the spherical shape of synthesized AgNPs, as spherical nanoparticles have only one oscillation mode of the surface plasmon [24]. The narrow FWHH obtained for solutions at pH less than 3 and greater than 7 indicates the presence of smaller nanoparticles with a size variation between 19.9 nm and 5 nm. However, in the pH range of 3–7, the spectra set showed broader bands that may result from aggregation of the nanoparticles in solution [15, 25].

The as-produced sols, specifically the yellow-colored silver, produced a characteristic absorbance peak at 386 nm, this wavelength of visible light creates a deep violet. From the UV-vis data, comparing the plasmon resonance wavelengths with the literature, the nanoparticles’ size can be estimated as being from 10 to 20 nm for the silver sols [24, 25].

3.3 Size distribution and Zeta potential

To evaluate the average size, size distribution, and possible aggregation of AgNPs, the DLS technique was used. Figure 3 exhibits the graphs from diameter depending on the differential number (%) at different pH values: 2.63, 3.60, 4.25, 5.90, 7.25, 8.07, and 9.05, respectively.

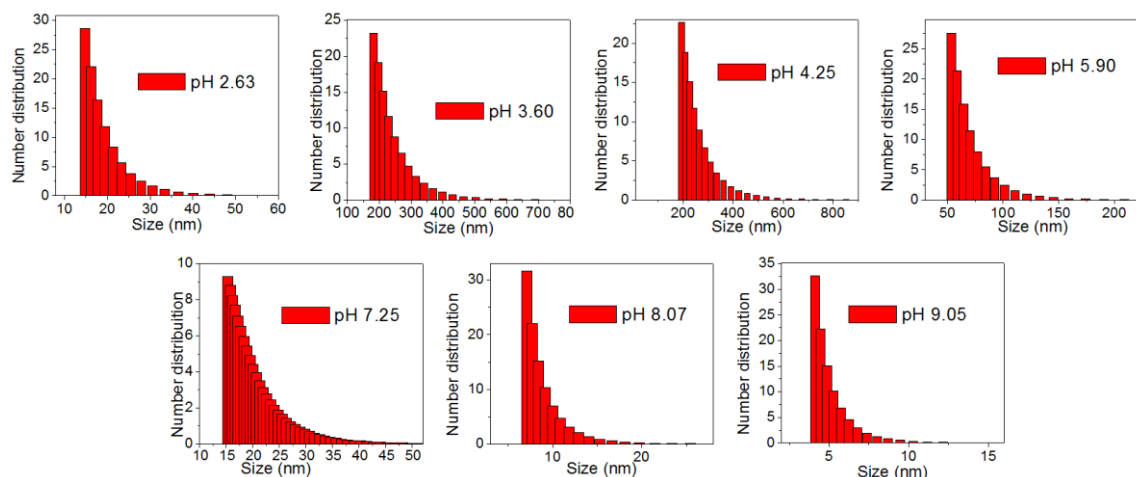


Figure 3: Diameter depending on the differential number (%) at different pH values: 2.63 (a), 3.60 (b), 4.25 (c), 5.90 (d), 7.25 (e), 8.07 (f), and 9.05 (g).

The size comparison showed that the solutions with pH less than 3 and greater than 7 have smaller nanoparticles, whereas, in the pH range 3–7, the nanoparticles have a larger size, which is consistent with a possible aggregation of the nanoparticles. The pH is directly related to the stability of the nanoparticles. The change in pH can alter the double-layer properties that can directly influence the zeta potential of the system, making the chances of flocculation or coagulation, because each type of nanoparticles is stable near the isoelectric point. AgNPs exhibited an effective charge change in aqueous conditions, from positive (in low pH) to negative (at high pH), with an isoelectric point between them, in which it presented a smaller size value [26].

The nanoparticles sizes are smaller than some related in the literature [21, 27, 28]. AJITHA *et al.* used the reduction method, pH between 6 and 12, however the smallest crystallite size was 14 nm [21]. The nanoparticles at pH less than 3 and greater than 7 are possibly less aggregated with a better colloidal stability of the solution. The colloidal stability of nanoparticles can be explained by a good adsorption of ligands on the surface of colloidal particles [29].

In this study, we used sodium citrate as a surface ligand, a salt from citric acid (2-hydroxy-1,2,3-propanetricarboxylic acid), which is a weak organic acid containing three ionizable groups whose pK_a values are 3.15, 4.77, and 6.40. Thus, below pH 3.15, the most part of their acid groups are protonated, resulting in a charge increasingly close to zero as the medium becomes more protonated [29]. To ascertain the interaction of the sodium citrate with the AgNPs as well as the aqueous medium, the surface charge of the nanoparticle systems was determined using zeta potential measurements.

Table 1 presents the zeta potential values and the average size of AgNPs as a function of pH.

Table 1. Zeta potential values and the average size of AgNPs as a function of pH.

pH	Zeta Potential (mV)	Size (nm)
2.63	12	18.7
3.60	-37	232
4.25	-66	249
5.90	-69	67.8
7.25	-66	19.9
8.07	-66	8.7
9.05	-61	5

It is observed that the value of the zeta potential is more positive at more acidic pH due to dissociation of some H^+ and total protonation of the carboxyl groups of sodium citrate, and at higher pH values there is an increase of OH^- ions in the dissociated solution and deprotonation of the carboxyl groups of citric acid gives a more negative zeta potential. As the lowest pK_a of citric acid is 3.15, the zeta potential values are coherent because at this pH all ionizable groups are protonated. This corresponds to the isoelectric point, and the zeta potential should be zero [30].

A minimum zeta potential of more than -30 mV is required for good physical stability, and of more than -60 mV for excellent stability [31]. Thus, from the zeta potential results, the silver colloidal solutions at pH greater than 4.25 are supposed to be less stable than at pH 2.63 or 3.6.

Figure 4 illustrates graphically the variation in the average size and zeta potential of AgNPs as a function of pH.

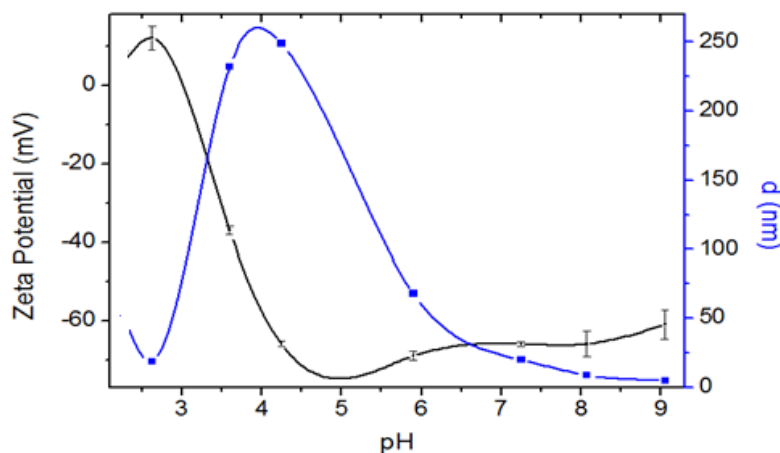


Figure 4: Variation in the zeta potential and average size of AgNPs as a function of pH.

In the pH range of 3–6, the nanoparticles are less stable, with larger sizes due to AgNP aggregation. This aggregation is due to the presence of electrostatic interactions between partially ionized sodium citrate groups. At the pH range lower than 3 and greater than 7, the AgNPs are less aggregated, because in pH lower than 3 all groups are protonated, working against the electrostatic interaction. Conversely, at pH greater than 7, all groups are deprotonated favoring the repulsion between the nanoparticles, which discourages their aggregation.

3.4 TEM Characterization

The AgNPs shape and size were studied by TEM operating at 200 kV. Figure 5 shows TEM images of the AgNPs prepared at pH 4.25 and 8.07. Samples prepared with pH 4.25 and 8.7 were selected for TEM measurement, due to the fact that they presented in one case agglomerated nanoparticles and in the other values indicating non-agglomeration of the material.

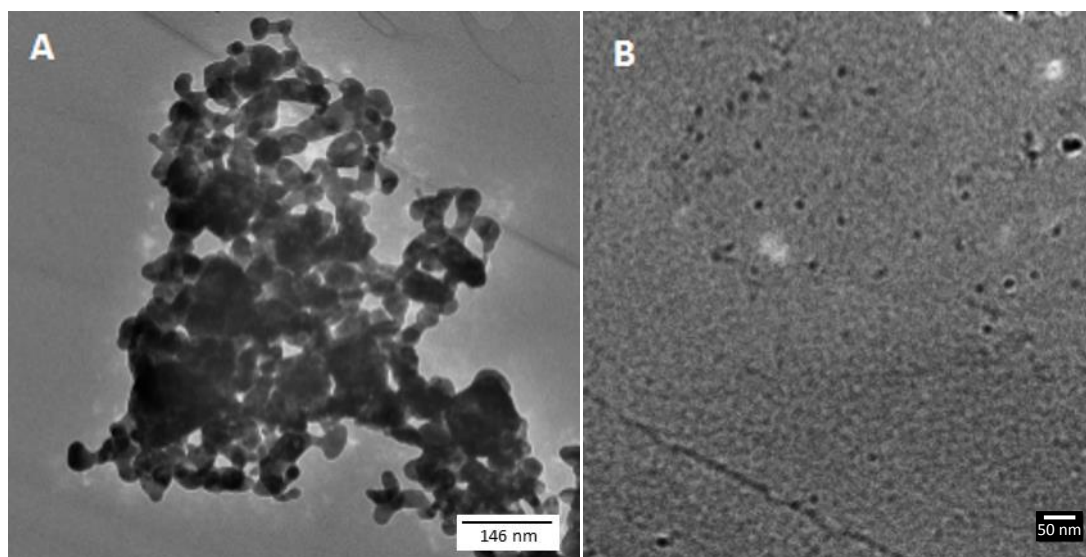


Figure 5: TEM images of AgNPs at pH 4 (A) and pH 8 (B).

The formation of roughly spherical nanoparticles can be confirmed by images in Figure 5, as observed in the UV-vis spectrum (Figure 4). The shape of the particles is not well defined but smaller particles have a spherical-like shape. The TEM image in Figure 5a shows nanoparticle agglomeration at pH 4.25, as observed by DLS, producing agglomerates with average sizes up to 249 nm, showing that in this condition the system is less stable. Figure 5b shows a TEM image of a sample obtained at pH 8.07; at this pH the nanoparticles are nonagglomerated, yielding nanoparticles that are more stable in these conditions. This result is in agreement with the data from DLS and zeta potential measurements; besides, Bastús *et al.* showed the roughly spherical shape and the fact that AgNPs formed were more agglomerated in lower pH, as in this case [32].

Thus, by using the techniques of characterization by UV-vis spectroscopy, DLS and zeta potential, and TEM, the AgNPs synthesis stabilized with sodium citrate was confirmed. The reaction conditions strongly influence the nanoparticles' shape and stability, and the pH was a determining factor in the stability and aggregation of nanoparticles.

3.5 Effect of AgNPs on bacterial growth

In this study, the size-dependent antimicrobial activity for AgNP samples was tested for three microorganisms. The AgNPs were prepared at pH 4.25 and 9.05, and their activity was analyzed by measurements of the ZOI. By this method, a greater ZOI correlates with a greater activity of AgNPs.

Samples with extreme values were selected for antimicrobial activity measurements. Samples with pH 4.25, with a reported size of 249 nm, and a sample with pH 9.05 with a size of 5 nm were selected. Table 2 summarizes the ZOI of disk diffusion tests of AgNP solutions prepared at pH 4.25 and 9.05, against Gram-negative (*Escherichia coli*) and Gram-positive (*Staphylococcus aureus*) bacteria and a fungus (*Candida albicans*).

Table 2. The ZOI values for different microbial strains as a function of AgNP solutions' pH.

Microbial strain	Control	AgNPs – pH 4 (mm)	AgNPs – pH 9 (mm)
<i>Candida albicans</i>	–	0.233 + 0.06	0.333 + 0.06
<i>Staphylococcus aureus</i>	–	0.167 + 0.06	0.333 + 0.06
<i>Escherichia coli</i>	–	0.167 + 0.06	0.333 + 0.11

The sample prepared at pH 4.25 exhibited agglomerated nanoparticles as already discussed, while the sample prepared at pH 9.05 exhibited smaller nanoparticles with no agglomeration. Both AgNP samples presented a small inhibition halo around the papers, proving that both samples had antibacterial activity. Bastús *et al.* also proved that at pH lower than 10, the AgNPs antibacterial effect is better 43 [30]. In contrast, Oukarroum *et al.* showed that the more acidic pH has a stronger cytotoxic effect on algal cells of *C. acidophila* 25 [18]. A quantitative analysis was performed by measuring in mm the ZOI around the papers. These results were obtained by subtracting the paper disk diameter from ZOI for all the microbial strains. No

significant differences were observed in the antimicrobial effect between the microbial strains tested, the greater antimicrobial activity is noticed for small nanoparticles.

4. CONCLUSIONS

In this study, AgNPs were synthesized by a chemical reduction method and the effect of pH on the colloidal stability of these nanoparticles was evaluated. The pH influence in the formation of AgNPs is extremely important. It was possible to characterize the formation of AgNPs stabilized with sodium citrate by means of UV-vis spectra, which showed a single band at 390 nm due to the spherical morphology of the nanoparticles and the surface plasmon resonance effect. From the TEM images, it was possible to confirm the morphology of spherical AgNPs, as well as its state of aggregation at different pH values. Moreover, through the variation of the pH, it was possible to observe a higher aggregation in the pH range between 3 and 7. At a pH lower than 3 and higher than 7, it was observed that there was less aggregation. From this study, we can confirm that the stability of AgNPs is highly influenced by pH. The synthesized AgNPs were found to have more antimicrobial potential than those described in earlier reports. The effect was more pronounced in smaller AgNPs obtained at higher pH values.

5. ACKNOWLEDGMENTS

The authors acknowledge the funding agencies CAPES, FAPEMIG and CNPq. This work is a collaborative research project of members of the Rede Mineira de Química (RQ-MG) supported by FAPEMIG (Project: CEX - RED-00010-14)

6. BIBLIOGRAPHY

- [1] SHU, M., HE, F., LI, Z., *et al.*, "Biosynthesis and Antibacterial Activity of Silver Nanoparticles Using Yeast Extract as Reducing and Capping Agents," *Nanoscale Research Letters*, n. 15v. 14, p. 9, 2020.
- [2] XIE, Y., YE, R., LIU, H., "Synthesis of silver nanoparticles in reverse micelles stabilized by natural biosurfactant," *Colloids and Surfaces A: Physicochemical and Engineering Aspects*, v. 279, n. 1-3, pp. 175-178, 2006.
- [3] ADELEKE OJO, O., OYINLOYE, B.E., BUSOLA OJO, A., *et al.*, "Green-route mediated synthesis of silver nanoparticles (AgNPs) from *Syzygium cumini* (L.) Skeels polyphenolic-rich leaf extracts and investigation of their antimicrobial activity," *IET Nanobiotechnology*, v. 12, n. 3, pp. 305-310, 2018.
- [4] SURIATI, G., MARIATTI, J., AZIZAN, A., "Synthesis of silver nanoparticles by chemical reduction method: Effect of reducing agent and surfactant concentration," *International Journal of Automotive and Mechanical Engineering*, vol. 10, no. December, pp. 1920-1927, 2014.
- [5] VARANDA, L.C., SOUZA, C.G.S., MORAES, D.A., *et al.*, "Size and shape-controlled nanomaterials based on modified polyol and thermal decomposition approaches. A brief review," *Annals of the Brazilian Academy of Sciences* 91(4): e20181180, 2019.
- [6] CHEN, Z., GAO, L., "A facile and novel way for the synthesis of nearly monodisperse silver nanoparticles," *Materials Research Bulletin*, vol. 42, no. 9, pp. 1657-1661, 2007.
- [7] ŠILEIKAITĖ, A., PROSYČEVAS, I., PUIŠO, J., *et al.*, "Analysis of Silver Nanoparticles Produced by Chemical Reduction of Silver Salt Solution," *Materials Science (Medžiagotyra)*, vol. 12, no. 4, pp. 1392-1320, 2006.
- [8] KUMAR, A., JOSHI, H., PASRICHA, R., *et al.*, "Phase transfer of silver nanoparticles from aqueous to organic solutions using fatty amine molecules," *Journal of Colloid and Interface Science*, vol. 264, no. 2, pp. 396-401, 2003.
- [9] PAL, A., SHAH, S., DEVI, S., "Synthesis of Au, Ag and Au-Ag alloy nanoparticles in aqueous polymer solution," *Colloids and Surfaces A: Physicochemical and Engineering Aspects*, vol. 302, no. 1-3, pp. 51-57, 2007.
- [10] LI, H., XIA, H., WANG, D., *et al.*, "Simple synthesis of monodisperse, quasi-spherical, citrate-stabilized silver nanocrystals in water," *Langmuir*, v. 29, n. 16, pp. 5074-5079, 2013.
- [11] CHAUDHARI, V.R., HARAM, S.K., KULSHRESHTHA, S.K., *et al.*, "Micelle assisted morphological evolution of silver nanoparticles," *Colloids and Surfaces A: Physicochemical and Engineering Aspects*, vol. 301, no. 1-3, pp. 475-480, 2007.
- [12] LIU, L., GAO, Z., JIANG, B., *et al.*, "Reversible Assembly and Dynamic Plasmonic Tuning of Ag Nanoparticles Enabled by Limited Ligand Protection," *Nano Letters*, p. acs.nanolett.8b02325, 2018.
- [13] SKIBA, M.I., VOROBYOVA, V.I., PIVOVAROV, A., *et al.*, "Green Synthesis of Silver Nanoparticles in the

Presence of Polysaccharide: Optimization and Characterization”, *Journal of Nanomaterials*, v. 2020, 10 p., ID 3051308, 2020.

- [14] RYCENGA, M., COBLEY, C.M., ZENG, J., *et al.*, “Controlling the Synthesis and Assembly of Silver Nanostructures for Plasmonic Applications,” *Chem Rev*, v. 111, n. 6, pp. 3669-3712, 2012.
- [15] HUSSAIN, J.I., TALIB, A., KUMAR, S., *et al.*, “Time dependence of nucleation and growth of silver nanoparticles,” *Colloids and Surfaces A: Physicochemical and Engineering Aspects*, v. 381, n. 1-3, pp. 23–30, 2011.
- [16] GOMATHI, M., RAJKUMAR, P.V., PRAKASAM, A., *et al.*, “Green synthesis of silver nanoparticles using *Datura stramonium* leaf extract and assessment of their antibacterial activity,” *Resource-Efficient Technologies*, v. 3, n. 3, pp. 280-284, Sep. 2017.
- [17] PERETYAZHKO, T. S., ZHANG, Q., COLVIN, V. L., “Size-Controlled Dissolution of Silver Nanoparticles at Neutral and Acidic pH Condition Kinetic and Size Changes,” *Environmental Science & Technology*, vol. 48, pp. 11954–11961, 2014.
- [18] OUKARROUM, A., SAMADANI, M., DEWEZ, D., “Influence of pH on the toxicity of silver nanoparticles in the green alga *Chlamydomonas acidophila*,” *Water, Air, and Soil Pollution*, v. 225, n. 8, 2014.
- [19] ALQADI, M.K., ABO NOQTAH, O.A., ALZOUBI, F.Y., *et al.*, “PH effect on the aggregation of silver nanoparticles synthesized by chemical reduction,” *Materials Science- Poland*, v. 32, n. 1, pp. 107–111, 2014.
- [20] NURFADHILAH, M., NOLIA, I., HANDAYANI, W., *et al.*, “The Role of pH in Controlling Size and Distribution of Silver Nanoparticles using Biosynthesis from *Diospyros discolor* Willd. (Ebenaceae),” *IOP Conference Series: Materials Science and Engineering*, v. 367, n. 1, 2018.
- [21] AJITHA, B., ASHOK KUMAR REDDY, Y., SREEDHARA REDDY, P., “Enhanced antimicrobial activity of silver nanoparticles with controlled particle size by pH variation,” *Powder Technology*, v. 269, pp. 110-117, 2015.
- [22] AGNIHOTRI, S., MUKHERJI, S., MUKHERJI, S., “Size-controlled silver nanoparticles synthesized over the range 5-100 nm using the same protocol and their antibacterial efficacy,” *RSC Advances*, v. 4, n. 8, pp. 3974–3983, 2014.
- [23] SHANKAR, S., CHORACHOO, J., JAISWAL, L., *et al.*, “Effect of reducing agent concentrations and temperature on characteristics and antimicrobial activity of silver nanoparticles,” *Materials Letters*, v. 137, pp. 160-163, 2014.
- [24] CSAPÓ, E., PATAKFALVI, R., HORNOK, V., *et al.*, “Effect of pH on stability and plasmonic properties of cysteine-functionalized silver nanoparticle dispersion,” *Colloids and Surfaces B: Biointerfaces*, v. 98, pp. 43-49, 2012.
- [25] MCFARLAND, A. D., HAYNES, C. L., MIRKIN, C. A., *et al.*, “Color My Nanoworld,” *Journal of Chemical Education*, v. 81, n. 4, p. 544A, 2004.
- [26] OĆWIEJA, M., MORGA, M., “Electrokinetic properties of cysteine-stabilized silver nanoparticles dispersed in suspensions and deposited on solid surfaces in the form of monolayers,” *Electrochimica Acta*, v. 297, pp. 1000-1010, 2019.
- [27] AJITHA, B., KUMAR REDDY, Y. A., REDDY, P. S., *et al.*, “Role of capping agents in controlling silver nanoparticles size, antibacterial activity and potential application as optical hydrogen peroxide sensor,” *RSC Adv.*, v. 6, n. 42, pp. 36171-36179, 2016.
- [28] GINJUPALLI, K., SHAW, T., TELLAPRAGADA, C., *et al.*, “Does the size matter? Evaluation of effect of incorporation of silver nanoparticles of varying particle size on the antimicrobial activity and properties of irreversible hydrocolloid impression material,” *Dental Materials*, pp. 1-8, 2018.
- [29] CHANDRAN, P.R., NASEER, M., UDUPA, N., *et al.*, “Size controlled synthesis of biocompatible gold nanoparticles and their activity in the oxidation of NADH,” *Nanotechnology*, v. 23, n. 1, 2012.
- [30] AL-GHAMDI, H.S., MAHMOUD, W. E., “One pot synthesis of multi-plasmonic shapes of silver nanoparticles,” *Materials Letters*, v. 105, pp. 62-64, 2013.
- [31] CHOUDHARY, R., KHURANA, D. KUMAR, A., *et al.*, “Stability analysis of Al₂O₃/water nanofluids,” *Journal Of Experimental Nanoscience*, vol. 12, n. 1 pp. 140–151, 2017.
- [32] BASTÚS, N., MERKOÇI, F., PIELLA, J., *et al.*, “Synthesis of Highly Monodisperse Citrate- Stabilized Silver Nanoparticles of up to 200 nm: Kinetic Control and Catalytic Properties,” *Chem. Mater.*, v. 26, n. MAY, p. 2836-2846, 2014.

ORCID

Leiriana Ap. P. Gontijo
Ellen Raphael
Daniela Pereira Santos
Jefferson Luis Ferrari
Juliana Pereira Lyon
Marco Antônio Schiavon

<https://orcid.org/0000-0003-2119-0272>
<https://orcid.org/0000-0002-5617-8428>
<https://orcid.org/0000-0003-3647-4139>
<https://orcid.org/0000-0002-1239-0988>
<https://orcid.org/0000-0002-9016-8311>
<https://orcid.org/0000-0002-1553-5388>